Bull Earthquake Eng
DOI 10.1007/s10518-011-9249-3

ORIGINAL RESEARCH PAPER

Seismic analysis of deep tunnels in near fault conditions: a case study in Southern Italy

Mirko Corigliano · Laura Scandella · Carlo G. Lai · Roberto Paolucci

Received: 3 August 2009 / Accepted: 6 February 2011

Abstract The importance of underground structures in transportation and utility networks makes their vulnerability to earthquakes a sensitive issue. Underground facilities are usually less vulnerable to earthquakes compared to above-ground structures, but the associated risk may be relevant, since even a low level of damage may affect the serviceability of a wide network. Seismic analysis of tunnels close to seismogenic faults is a complex problem, which is often neglected at the design stage for the lack of specific codes or guidelines for the design of underground structures in seismic conditions and also because, as mentioned above, underground structures are considered less vulnerable to earthquake loading. This paper investigates the seismic response of deep tunnels focusing on the required steps for a proper design under both static and dynamic loading. The study aims at contributing to improve the methods currently used for the seismic analysis of underground structures. At this purpose, the seismic response of a deep tunnel in Southern Italy has been investigated along the transversal direction. The infrastructure is part of the railway switch line connecting Caserta to Foggia in the Southern Apennines which is one of the most active seismic regions in Italy. The seismic response in the transversal direction has been analysed by using the pseudo-static approach as well as through advanced numerical modeling using the spectral element method coupled with a kinematic approach for finite fault simulations. The pseudo-static approach has been implemented using a closed-form analytical solution.

M. Corigliano (✉) · L. Scandella · C. G. Lai
European Centre for Training and Research in Earthquake Engineering, EUCENTRE, Via Ferrata 1, CAP 27100, Pavia, Italy
e-mail: mirko.corigliano@eucentre.it

L. Scandella
e-mail: laura.scandella@eucentre.it

C. G. Lai
e-mail: carlo.lai@eucentre.it

R. Paolucci
Politecnico di Milano, Department of Structural Engineering, P.za Leonardo da Vinci, CAP 20133, Milan, Italy
e-mail: roberto.paolucci@polimi.it

Published online: 05 March 2011

The results obtained from advanced numerical modeling and the pseudo-static method have been compared to assess their validity and limitations.

Keywords Deep tunnels · Seismic analysis · Soil-structure interaction · Near-fault conditions · Spectral element method

1 Introduction

Underground structures are critical elements in transportation and utility networks (e.g. railway and road tunnels, hydraulic tunnels and hydroelectric caverns, lifelines for transportation of water, oil, natural gas, etc.). Their seismic response is considerably different from that of the corresponding above-ground facilities. Since the relative movement of pipes and tunnels with respect to the surrounding soil is generally small, the structural response is dominated by the surrounding soil behaviour. The inertia forces due to the weight of the structure are often negligible compared to the mass of the surrounding ground, and the stress confinement provides high values of radiation damping. It is a fact that underground facilities are in general less vulnerable to earthquakes in comparison with above-ground infrastructures (Barton 1984; Ates et al. 1995). Nevertheless, several tunnels and underground structures suffered severe damages, especially during strong earthquakes such as the recent 1995 Kobe (Japan), 1999 Chi-Chi (Taiwan) and 2004 Niigata (Japan) events. A review of damages suffered by underground structures during these events shows that most tunnels were located in the vicinity of causative faults. This condition implies a high factor of risk since ground motion may be characterized by strong and coherent long period pulses. Therefore, a careful definition of the seismic input for the seismic assessment of these structures is required.

The static design of tunnels nowadays has achieved a high level of refinement, mainly due to the availability of sophisticated numerical methods which allow one to simulate all construction phases (such as excavation), cast in place of temporary reinforcement and modelling of the complex boundary conditions. A similar level of accuracy is not yet developed for the estimation of stress increments in tunnel linings due to earthquake loading. This is partly due to the fact that tunnels are not considered very sensitive to earthquakes, and only few code prescriptions and guidelines specifically address the issue of seismic design (e.g. ISO 23469 2005 and the French AFPS/AFTES 2001).

This paper aims at analyzing the seismic response of deep tunnels in near field conditions and to introduce improved approaches for the seismic design of underground structures. This is achieved by means of both simplified methods and advanced numerical simulations with the goal of assessing advantages and limitations of approaches characterized by different levels of refinement. The attention will be specifically devoted to the steps implemented in the design of deep tunnels under earthquake loading, namely:

(i) characterization of rock mass for stress analysis under static conditions;
(ii) static analysis;
(iii) definition of seismic input in near-field conditions;
(iv) stress analysis under seismic loading;
(v) superposition of static and dynamic loading effects.

The proposed procedure will be applied to a real case study, the Serro Montefalco tunnel located in Southern Italy. The infrastructure is part of the railway switch line connecting Caserta to Foggia, in the Northern sector of the Southern Apennines, one of the most seismically

active regions in Italy. The paper, after a brief description of the geological and seismological setting of the case study, illustrates the methods adopted for the definition of the seismic input required for dynamic analyses of the tunnel considering the transverse response. Special attention has been devoted to the evaluation of strains, which dominate the seismic response of underground structures, such as tunnels or pipelines.

The method of Hisada and Bielak (2003) has been adopted to generate synthetic time histories of earthquake ground motion, based on an extended kinematic fault model. The synthetic seismograms have been used to assess tunnel response via advanced numerical analyses as well as for the evaluation of the maximum shear deformation induced within the tunnel, as required by simplified approaches.

Since the assessment of the seismic behaviour of a tunnel along the transversal direction requires the knowledge of the internal forces acting on the lining prior to the earthquake, static analyses simulating the evolution of the state of stress during all phases of construction of the tunnel have been performed using FLAC (Itasca 2005), a well-known finite difference-based computer program.

Subsequently, the stress increment in the lining due to the seismic excitation has been calculated and compared using a pseudo-static approach and advanced numerical modeling. Numerical analysis has been carried out using GeoELSE (Geo Elastodynamics by Spectral Elements, http://geoelse.stru.polimi.it/), a spectral element-based computer program coupled with GRFLT, a computer code developed by Hisada and Bielak (2003) for finite fault simulations. The coupling has been implemented through the use of the Domain Reduction Method (Bielak et al. 2003; Scandella 2007; Stupazzini et al. 2006). The pseudo-static approach has been implemented using a closed-form analytical solution developed by Corigliano et al. (2006).

2 Case study: the Serro Montefalco tunnel

The new "*Caserta-Foggia"* railway line is part of the doubling of the original route representing one of the most important crossings of the Apennines, in Southern Italy. The new railway line was designed in the late 80's and includes 17 tunnels. The line between Caserta and Apice (close to Benevento) was built in the early 90's whereas for the last part of it only a preliminary design has been carried out.

The "*Serro Montefalco*" tunnel belongs to the final section of the "*Caserta-Foggia*" line. This is a 11.7 km long tunnel with a maximum cover of 225 m. It represents one of the most relevant structures of the entire railway line due to the complexity of the geological setting (see Fig. 1b). The lithotypes include varicoloured clay-shales, marl and marly limestone, clay and marl intercalated with limestone (Barla et al. 1986). The varicoloured clay-shales (the so-called "*Argille Scagliose*") include expansive clay minerals, which exhibit a significant swelling behaviour. Previous excavations of tunnels (e.g. the "*San Vitale*" Tunnel) in these weak rock formations (see Barla et al. 1986 and Lunardi and Bindi 2004 for more details) presented severe squeezing and swelling problems leading to face instability, large convergences, invert-heave and critical loading of the tunnel support.

The "*Serro Montefalco*" tunnel has been chosen as case study due to the relevant seismicity of the region and the availability of the design data. The Southern Apennines are characterized by a narrow seismic belt NW-SE-striking and approximately 30–50 km wide, which follows the axis of the chain (Improta et al. 2000). The Northern sector of the Southern Apennines, the "Sannio" region, where the "Serro Montefalco" tunnel is located, is one of the most active seismic territories in Italy. This area in the last three centuries was struck by

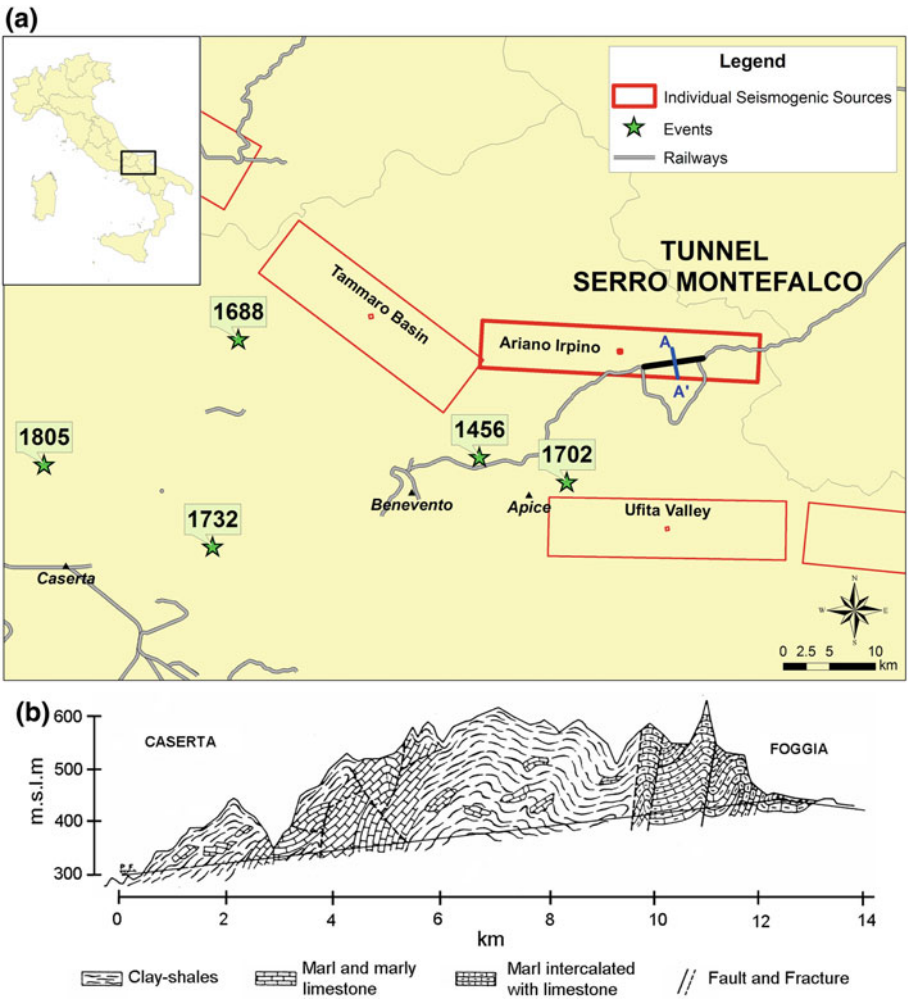

Fig. 1 **a** Location of the "Serro Montefalco" tunnel (*thick line*) along the *Caserta-Foggia railway line* (*gray line*) in the Sannio region. Epicentres of the most destructive earthquakes in the last three centuries (*stars*) are shown. The active faults (from the DISS 3.0.2 (2006) database) close to the tunnel are superimposed; the Ariano Irpino fault used as seismic source in the dynamic analysis is highlighted. The *thin line* A–A' shows the representative modelled cross-section of the tunnel. **b** Geological profile along the *Caserta-Foggia line*, where the "Serro Montefalco" tunnel is located (from Barla et al. 1986)

four large destructive earthquakes occurred in 1688 (IMCS = XI), 1702 (IMCS = X), 1732 (IMCS = X), and 1805 (IMCS = X), as shown in Fig. 1a. Since 1805, a period of seismic quiescence followed. At present, the seismicity is characterized by low-energy earthquakes frequently clustered in swarms which occur at the borders of primary faults that are sources of the most energetic earthquakes (Improta et al. 2000). Due to this long quiescence, the Sannio region is expected to experience in the near future a strong and destructive seismic event.

3 Seismic ground strains in near-fault conditions

It is well known that long infrastructures, such as viaducts, pipelines and tunnels, require a careful selection of the seismic input to account for the spatial variability of ground motion, especially in near-fault conditions, where the motion may strongly depend on the complex coupling of the seismic source, rupture process, source-site travel path and local site conditions (Stupazzini et al. 2009). Consequently, the features of ground motion in the proximity of an active fault can be significantly different from those in the far-field. There is no well defined distance over which a site may be classified as in near or far-field. A useful criterion to define the near-field zone is based on the comparison of the source dimension with the source to site distance. Experience shows that only at distances smaller than $15 \div 25$ km relevant damage to underground facilities is expected to occur.

Since the seismic response of underground structures is dominated by the surrounding ground deformation and not by the inertial properties of the structure itself, the standard representation of the seismic input in terms of response spectral ordinates is not suitable. Instead, the dynamic analysis of the structure should be carried out using three components time histories of ground motion. According to Eurocode 8 Part 1 (EN 1998-1, 2004), acceleration time histories can be defined using different approaches including artificial spectrum-compatible accelerograms, synthetic records generated by a seismological model of the source or real accelerograms. However, the use of artificial spectrum-compatible accelerograms for geotechnical applications is not allowed by the EC8 and also by the recent Italian building code (NTC 2008).

In spite of the availability of large digital accelerometric databases in many seismically active regions of the world, relatively few good quality strong motion records are available in near-fault conditions. Almost none at depth below the ground level. These would be useful to define the seismic input for an underground structure located close to a seismogenic fault.

Therefore, to define a suitable seismic input for the problem under study, two approaches have been adopted, namely:

- generation of synthetic time series using the method by Hisada and Bielak (2003), which simulates the seismic source as an extended kinematic fault (see Sect. 3.1);
- simplified evaluation of the rock Peak Ground Strain (*PGS*) for simplified pseudo-static analyses (see Sect. 3.2).

3.1 Seismic ground motion by finite fault numerical simulations

To provide a suitable seismic input for dynamic analyses of the tunnel, finite fault numerical simulations have been performed using the method proposed by Hisada and Bielak (2003) that simulates the complete 3D seismic wavefield induced by an extended kinematic fault coupled with a horizontally layered crustal model. This approach allows to investigate the effects of the source, fling step, rupture directivity and strong motion in near-fault conditions, which may play a relevant role in the expected ground shaking.

Proper definitions of the seismic source model and of the crustal profile along the whole propagation path are required for the application of the method.

3.1.1 Source model

The Italian Database of Individual Seismogenic Sources (DISS 2006) indicates three relevant faults close to the "Serro Montefalco" tunnel: the *Ariano Irpino*, *Ufita Valley* and *Tammaro*

Table 1 Main parameters of the Ariano Irpino fault (from DISS V3.0.3 2006)

Seismic moment	2.54×10^{19} Nm	Strike	277°
Moment magnitude	6.9	Dip	70°
Min. depth	11 km	Rake	230°
Max. depth	25 km	Length	30.0 km
Hypo. depth	22.7 km	Width	14.9 km
Rise time	1.8 s	Slip	2.0 m
Rupture velocity	2.8 km/s	Max freq.	5 Hz

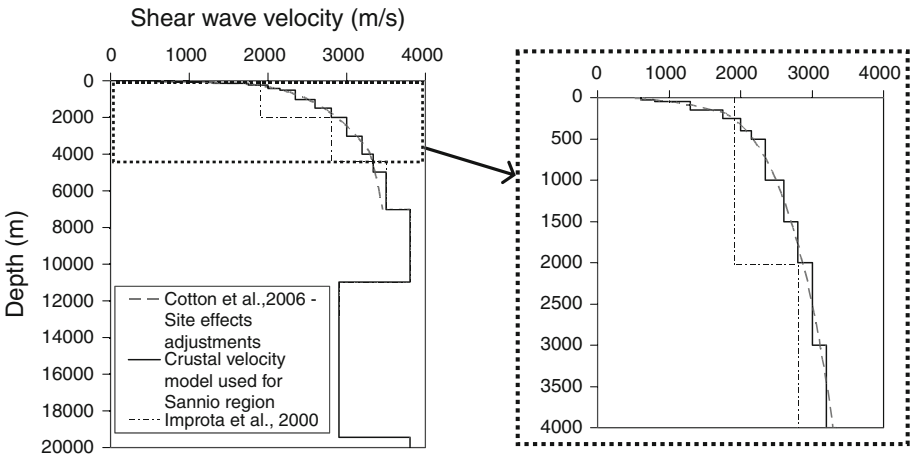

Fig. 2 Crustal velocity profile (S wave) adopted for the numerical model

Basin faults all of which are shown in Fig. 1a. The Ariano Irpino fault has been selected as the reference seismic source, because it is the closest to the tunnel and it is capable of a M_w 6.9 earthquake. It was the source of the December 5, 1456 earthquake, one of the most important natural events of the Italian seismic history. The main features of this source and the parameters adopted for the deterministic simulation are listed in Table 1.

3.1.2 Crustal velocity model

To define a crustal velocity profile for application of the Hisada and Bielak (2003) method, the Improta et al. (2000) model was considered for the deeper part, which is based on the interpretation of seismic refraction data and of several sonic velocity logs obtained from oil wells in the region surrounding the area of study. To provide a more realistic shallow velocity profile, we have adopted within the first 5 km from ground surface the rock model proposed by Cotton et al. (2006), assuming $V_{S30} = 600$ m/s. The resulting layered crustal model is shown in Fig. 2 and the material properties adopted in the numerical model are listed in Table 2.

3.2 Evaluation of ground strain field

As mentioned above, the seismic response of underground structures is dominated by earthquake-induced deformation of the surrounding soil. Since direct measures of earthquake-induced ground strains are generally not available, and since the ground deformation

Table 2 Material properties assumed for the layered crustal model used for the Ariano Irpino fault ground motion simulations

Layer	ρ [t/m^3]	V_P [m/s]	V_S [m/s]	Q_P –	Q_S –	Depth [m]	Thickness [m]
1	1.80	1,039	600	60	30	from 0 to 25	25
2	1.90	1,386	800	100	50	from 25 to 50	25
3	2.10	2,252	1,300	150	75	from 50 to 150	100
4	2.30	3,031	1,750	200	100	from 150 to 250	100
5	2.35	3,464	2,000	200	100	from 250 to 400	150
6	2.40	3,724	2,150	200	100	from 400 to 500	100
7	2.40	4,070	2,350	260	130	from 500 to 1,000	500
8	2.50	4,503	2,600	300	150	from 1,000 to 1,500	500
9	2.55	4,850	2,800	320	160	from 1,500 to 2,000	500
10	2.55	5,196	3,000	320	160	from 2,000 to 3,000	1,000
11	2.60	5,543	3,200	320	160	from 3,000 to 4,000	1,000
12	2.60	5,785	3,340	320	160	from 4,000 to 5,000	1,000
13	2.70	6,062	3,500	400	200	from 5,000 to 7,000	2,000
14	2.70	6,582	3,800	500	250	from 7,000 to 11,000	4,000
15	2.55	5,023	2,900	320	160	from 11,000 to 19,150	8,450
16	2.70	6,582	3,800	500	250	from 19,450 to ∞	–

pattern in realistic geological and tectonic conditions is hard to predict, it is customary in the engineering practice to make use of simplified formulas.

The Peak Ground Strain (*PGS*) is related to the Peak Ground Velocity (*PGV*) by means of the following relation (Newmark 1967):

$$PGS = \frac{PGV}{C} \tag{1}$$

where *PGS* may refer to either the longitudinal or the shear deformation. The parameter *C* (dimensionally is a velocity) is defined in terms of the apparent speed of propagation of the dominant phases of seismic motion, either body or surface waves, with values typically ranging from 2 and 5 km/s (O'Rourke 2003). As discussed in several papers (see e.g. Zerva 2003; Paolucci and Pitilakis 2007; Paolucci and Smerzini 2008; Scandella and Paolucci 2010), the practical application of Eq. (1) may be limited especially when the simplifying assumption on which this relation is based (i.e. of a seismic wavefield consisting of plane waves propagating in a homogeneous medium) is not applicable. Therefore, in this work we have calculated ground strains based on the kinematic modeling of the seismic source described in Sect. 3.1. The maximum earthquake-induced ground strain was calculated by numerical differentiation of the computed numerical displacement time histories $v(y, z)$ and $w(y, z)$ at four points around the cross-section of the tunnel (Corigliano et al. 2006), as shown in Fig. 3. Denoting by "x" the longitudinal axis of the tunnel, the shear strain γ_{yz} have been computed as follows:

$$\gamma_{yz} = \frac{\partial v}{\partial z} + \frac{\partial w}{\partial y} \cong \frac{1}{2\,\Delta z}\left[v\,(y_o, z_o + \Delta z) - v\,(y_o, z_o - \Delta z)\right] + \frac{1}{2\,\Delta y}\left[w\,(y_o + \Delta y, z_o) - w\,(y_o - \Delta y, z_o)\right] \tag{2}$$

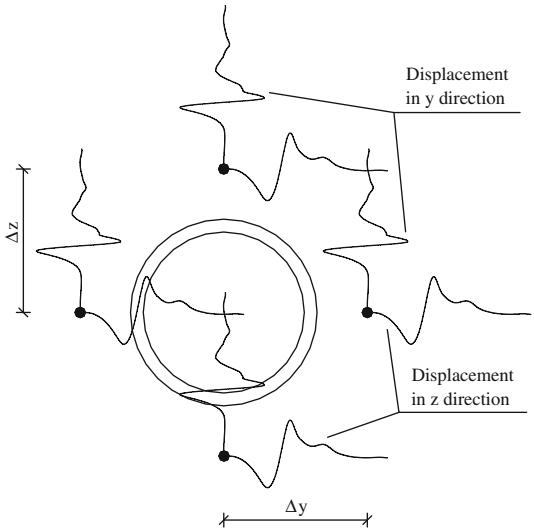

Fig. 3 Displacement time histories evaluated by the Hisada and Bielak (2003) method in free-field conditions at the tunnel depth in 4 points around the tunnel

where the partial derivatives have been computed using the second order, central finite difference operators, v and w are the ground displacement in y and z direction, Δy and Δz are the spacings between two points considered in y and z directions.

4 Response along the transversal direction of the tunnel

The seismic response of a representative transversal cross-section of the Serro-Montefalco tunnel has been analyzed. Special attention has been devoted to the ovaling, which is one of the most critical deformation patterns induced by ground shaking to a tunnel lining (Hashash et al. 2001). The estimation of the seismic stress in the lining requires a preliminary calculation of the static stresses acting prior to the earthquake loading. In this study, after the static analysis, the seismic response has been analysed by two approaches: a fully dynamic analysis and a pseudo-static approach. In both approaches, the free-field ground strains have been calculated as illustrated in the previous section, to provide a meaningful comparison and a cross-validation of the two methods.

The main scope of the static analysis is the reproduction of the stress in the lining due to the excavation and construction stages of the tunnel. On the other hand, dynamic analyses aim at evaluating the stress increment in the lining due to the seismic wave propagation.

It is important to remark that the geotechnical parameters used under static and dynamic loading are different, due to the different level of deformation involved. Static parameters have been defined on the basis of the standard methods used in rock mechanics, whereas in the dynamic analysis elastic moduli at low strains were used. In both static and dynamic analyses, the rock mass has been modelled as an isotropic, linear elastic continuum since the influence of discontinuities in weak rocks can be neglected.

4.1 Static analysis

A set of static analyses have been carried out to properly simulate the construction stages of the tunnel and to compute cross-sectional internal forces in the lining prior to the earthquake

Table 3 Strength and deformability parameters of varicoloured clay-shales (Barla et al. 1986)

Cohesion	50 kPa
Friction angle	22°
Young's modulus	200 MPa
Poisson ratio	0.45

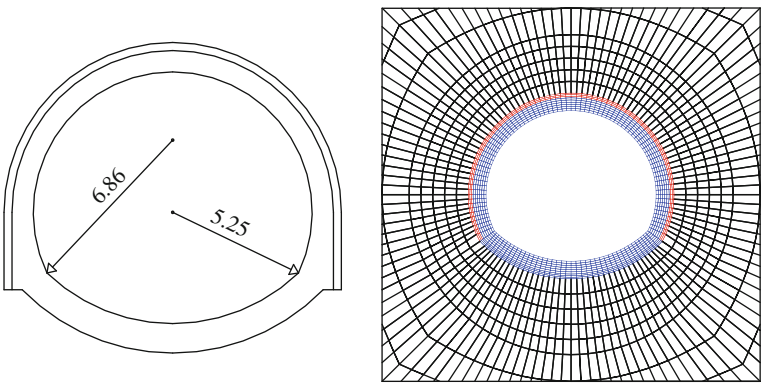

Fig. 4 **a** Cross-section of the "Serro Montefalco" tunnel; **b** mesh of the FLAC model

loading. The parameters of the rock mass along the tunnel length have been defined on the basis of geomechanical classification and scaling rules of the intact rock properties obtained from laboratory tests.

For soil-like materials (e.g. varicoloured clay-shales) reference was made to laboratory tests conducted on undisturbed samples (e.g. triaxial tests, direct shear tests, consolidation tests, etc.) obtained from borehole drilling and from a limited number of field investigations such as flat-dilatometer tests (Barla et al. 1986). The strength and deformability parameters adopted for the varicoloured clay-shales formation are listed in Table 3.

Static analyses have been performed using the finite difference-based code FLAC (Itasca 2005). A two-dimensional model of the tunnel under plane strain conditions (Fig. 4b) has been constructed. In order to simulate the excavation stages, which determine 3-D stress-strain conditions near the tunnel face, the stress relaxation method proposed by Panet (1995) has been used. This introduces a fictitious stress $(\sigma)_c$ acting on the two-dimensional model as follows:

$$(\sigma)_c = (1 - \lambda)\ (\sigma)_p \tag{3}$$

where λ is the stress relaxation factor ranging between 0 and 1 depending on the distance of the cross-section from the tunnel face, and $(\sigma)_p$ is the geostatic state of stress.

Calculations have been performed with reference to a geostatic stress in the rock mass given by an overburden pressure $\sigma_v = 2.14$ MPa (which corresponds to a depth of approximately 100 m) and with *at-rest* stress coefficient $K_0 = 0.8$ (Barla et al. 1986), where K_0 is the ratio between the effective horizontal stress σ'_h and the effective vertical stress σ'_v.

The rock mass has been modelled using an elastic-perfectly-plastic constitutive law, based on the Mohr-Coulomb yield criterion and a non-associated flow rule. The construction stages have been simulated through the following steps:

Table 4 Mechanical parameters of the primary support

Shotcrete	Thickness = 30 cm	$\nu = 0.2$	$E_{shot} = 4{,}000$ MPa
Steel ribs HEB200	$A_{steel} = 78.1\,cm^2$ $J_{steel} = 5{,}696\,cm^4$	D = 1.0 m	$E_{steel} = 210{,}000$ MPa
Equivalent parameters	G = 3,932 MPa K = 5,243 MPa	$\nu = 0.2$	$E_{eq} = 9{,}438$ MPa

Table 5 Mechanical parameters of final lining

E	γ	ν	K	G	Thickness at the crown	Thickness at the invert
30 GPa	$25\,kN/m^3$	0.2	16.67 GPa	12.50 GPa	80 cm	110 cm

- simulation of the initial geostatic stress;
- full face excavation up to a 50% removal of the stress on the tunnel profile;
- application of the primary support at the crown and closure of the ring by the reinforced concrete lining installed at the invert;
- additional removal up to 75% of the initial stress on the tunnel profile, with the above support system installed;
- installation of final concrete lining at the crown and complete relaxation of the stress on the tunnel profile;
- degradation of the geotechnical parameters of the primary support.

The primary support consists of a ring of a 30 cm thick shotcrete layer and steel ribs (1 HEB 200 per meter). It has been modelled by plane strain elements with a linear elastic isotropic behaviour, characterized by an equivalent Young's modulus (Oreste 1999). The elastic parameters used for the primary support are listed in Table 4.

The final reinforced concrete lining, which acts as a permanent structural support of the tunnel, will carry both the whole static load and the additional dynamic loading increment caused by the earthquake. A typical cross-section of the tunnel located in the varicoloured clay-shales formation, which includes the primary and final lining, is shown in Fig. 4a. The final reinforced concrete lining has been idealized using linear elastic, isotropic plane strain elements (see Fig. 4b) with the elastic parameters reported in Table 5. The cross-sectional forces acting along the lining are shown in Figs. 5 and 6.

Figure 5 shows that the state of stress in the lining is governed by the stress increment induced during the construction stages, which includes the cast in place of the invert, the primary support close to the tunnel face and the closure of the crown. The sequence of the construction stages generates in the final step large bending moments at the invert with stresses approaching the limit design values for the cross-section (see Fig. 6b). Thus, underground structures excavated in complex geological/geotechnical settings, like the "*Serro Montefalco*" tunnel, may undergo significant damages if an additional loading increment (such as that due to an earthquake) is superimposed (Corigliano et al. 2007).

A similar situation occurred in Turkey to the Bolu tunnel, which crosses the North Anatolian Fault and was severely damaged due to the M_w 7.1 Düzce earthquake of November 12, 1999 (Erdik 2000).

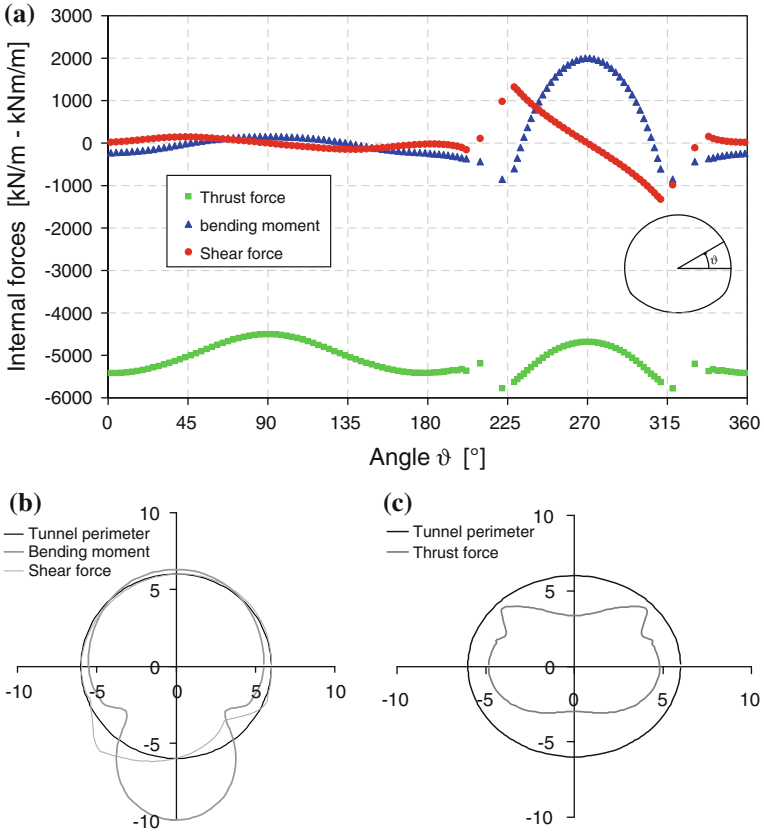

Fig. 5 **a** Cross-sectional forces acting on the reinforced concrete lining at the final stage of construction: thrust force (*triangles*); bending moment (*diamonds*) and shear force (*circles*); **b** Bending moment and shear force along the tunnel perimeter; **c** Thrust force along the tunnel perimeter

4.2 Advanced dynamic modeling

Advanced numerical analyses have been performed to assess the dynamic response of the tunnel cross-section during seismic loading. These include simultaneous consideration of seismic source, propagation path, geological site conditions, the effects of dynamic soil-structure interaction. The analyses have been carried out using GeoELSE (Geo-ELastodynamics by Spectral Elements, http://geoelse.stru.polimi.it), a spectral element-based computer program jointly developed at the Department of Structural Engineering of Politecnico di Milano (Faccioli et al. 1997) and at CRS4 (Center for Advanced Studies, Research & Development in Sardinia, Italy). GeoELSE is a powerful computer program implemented in a parallel architecture (Stupazzini et al. 2009) that has been specifically designed to solve complex wave propagation and dynamic soil-structure interaction problems.

GeoELSE capabilities were further enhanced by the implementation of the Domain Reduction Method (Bielak et al. 2003; Scandella 2007), a powerful substructuring approach which reduces the computational cost required in the numerical analysis of large scale dynamic soil-structure interaction problems. The main idea behind DRM is the subdivision of the

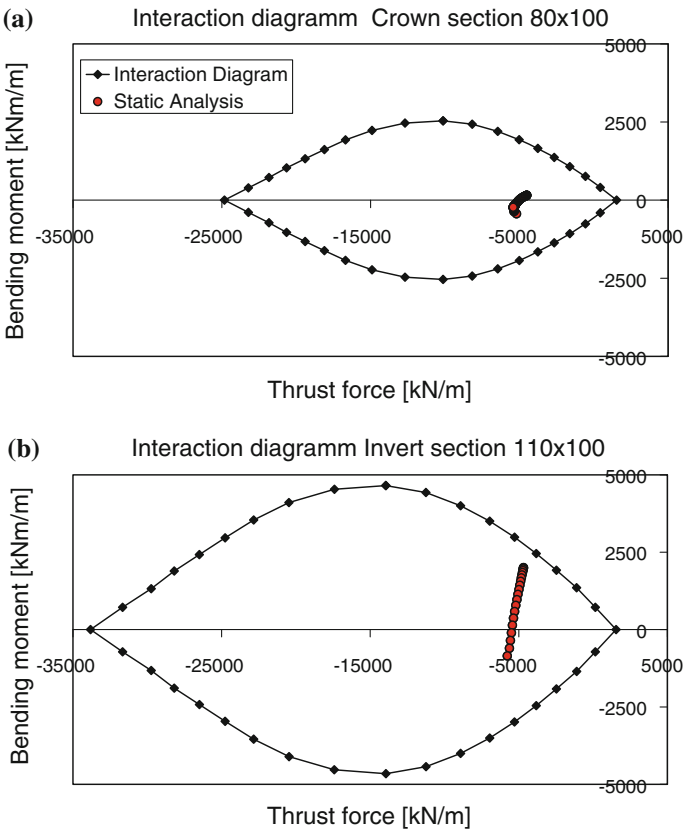

Fig. 6 Interaction diagrams (*solid line with squares*) for the tunnel cross-section in static condition (*circles*): **a** crown section 80 × 100; **b** invert section 110 × 100

original problem into two simpler subproblems, solved in two sequential steps, as illustrated in Fig. 7. Step 1 (see Fig. 7a) simulates the seismic response of the free-field (*auxiliary*) problem, consisting of the wave propagation generated by a seismic source placed inside a medium (*external domain*) from which the structure has been removed and replaced by the same material as the surrounding soil. Step 2 (see Fig. 7b) involves the numerical solution of the *reduced* problem involving the structure alone (in this case, the tunnel) and only a reduced portion of the surrounding soil (*internal domain*). Therefore, the DRM allows to perform an exact coupling between a large scale external domain, involving the seismic source, but excluding the structure, and an internal small-scale domain, including the structure, but excluding the source of the excitation. As shown by Bielak et al. (2003), the input for Step 2 of DRM is a set of effective nodal forces evaluated on the basis of the ground displacement calculated in the Step 1 and applied in a strip of elements (dark boundary in Fig. 7). These forces are equivalent to and replace the original seismic forces applied in the first step to reproduce the seismic source. A detailed description of the implementation of the DRM applied to Spectral Elements can be found in Faccioli et al. (2005) and Scandella (2007).

In this study the auxiliary problem (external domain) has been solved using the GRFLT program developed by Hisada and Bielak (2003) (see Sect. 3.1) assuming a layered crustal

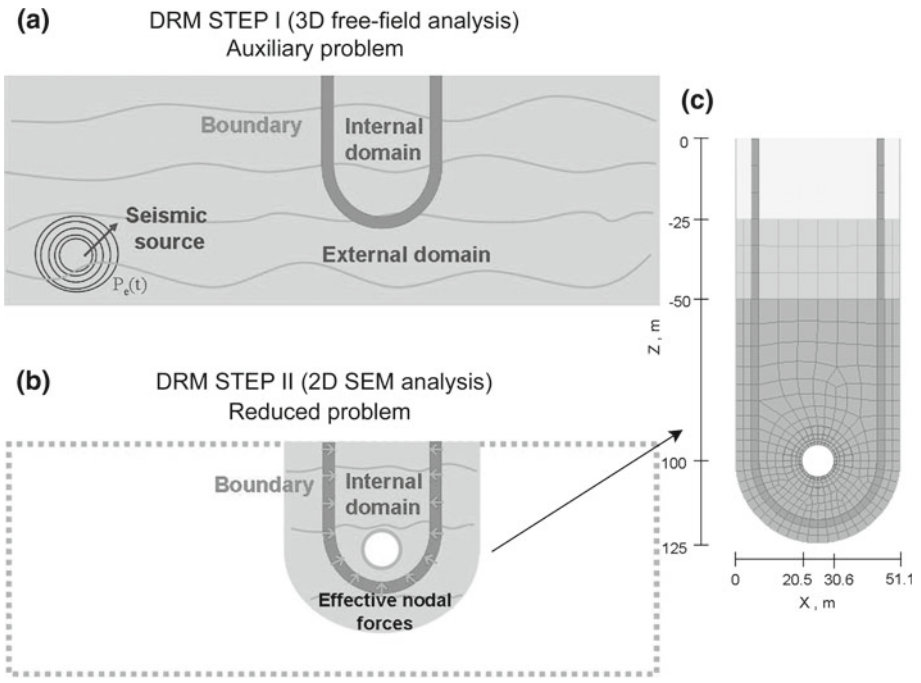

Fig. 7 DRM procedure applied to the case study. **a** Step I: free-field analysis of the wave propagation from the seismic source; **b** Step II: wave propagation in the reduced domain including soil-structure interaction. The *dark line* denotes the effective boundary. **c** SE model of the reduced problem including the transversal A–A' cross-section of the tunnel

model with properties illustrated in Table 2. The results of the analyses are shown in Fig. 3 in terms of displacement time histories at selected nodes. As expected, the seismic motion does not vary significantly at the various nodes around the tunnel due to the wavelengths propagated that are large with respect to the dimensions of the structure. However, the spatial variability of the displacement field induced by wave propagation effects generates a significant deformation field, as it will be shown in the next sections.

As a second important remark, it should be noticed that, although the numerical simulation with GeoELSE was set to propagate frequencies up to 5 Hz, the modelling of the seismic source through the GRFLT program allowed to reproduce the radiation of energy at frequencies not exceeding 2 Hz. Therefore, the magnitude of the deformation field reproduced by the numerical simulations could be underestimated.

Step 2 of the DRM has been solved applying GeoELSE to a 2D numerical model of the cross-section A–A' of the "*Serro-Montefalco*" tunnel shown in Fig. 1a. A circular cross-section of the tunnel was adopted with an equivalent external radius of 5.85 m and a concrete lining thickness of 0.80 m. This simplified the geometry for the numerical modeling and allowed to compare the results with those obtained with the pseudo-static approach.

The Young's modulus and Poisson's ratio adopted for the lining are shown in Table 5. The SEM model of the reduced problem, shown in Fig. 7c, has the mechanical properties shown in Table 6. A no slip condition has been assumed at the interface between the soil and the lining, as further discussed in the next section.

The maximum dynamic increment of the axial force and of the bending moment obtained from advanced numerical modeling will be compared with the results obtained by a simplified

Table 6 Dynamic properties adopted for the reduced model in the advances numerical analyses

Layer N.	V_S (m/s)	V_P (m/s)	ρ (kg/m^3)	Q_S (–)
1	600	1,039	1,800	30
2	800	1,386	1,900	50
3	1,300	2,252	2,100	75
Tunnel	2,236	3,651	2,500	80

closed-form solution derived using a pseudo-static approach, taking into account soil-structure interaction effects in no-slip conditions.

4.3 A closed-form solution for simplified pseudo-static analysis

A simplified pseudo-static analysis of the transversal cross-section of the tunnel has been performed applying the closed form solution developed by Corigliano et al. (2006). The approach considers a lined circular tunnel (diameter 5.85 m and thickness 0.80 m) under plane strain conditions. The rock mass is considered to be an infinite, linear-elastic, homogeneous, isotropic medium. The tunnel lining is modeled as an elastic cylindrical shell in plane strain conditions.

Since the real boundary conditions at the soil-structure interface are unknown, simplified solutions available in the literature for the evaluation of seismic actions generally consider two extreme cases which bound the real situation: the *full-slip* and the *no-slip* conditions. In the engineering practice the two analytical solutions proposed by Wang (1993) and Penzien (2000) are widely used for the evaluation of the dynamic stress increment in the tunnel lining. The two solutions provide the same result for the *full-slip* condition, but the solution proposed by Penzien (2000) underestimates the thrust force in the *no-slip* case. This aspect was observed by Hashash et al. (2005) while studying the problem with Finite Elements (FE) numerical analyses and it was confirmed also by Kontoe et al. (2008), who compared FE numerical results with the simplified analytical solutions calculated for the Bolu tunnels, which experienced extensive damage after the 1999 Düzce earthquake. On the other hand, Hashash et al. (2005) showed that the solution by Wang (1993) leads to correct results. This has also been confirmed by the analytical solutions independently developed by Corigliano et al. (2006) which will be briefly recalled hereinafter.

A full-slip condition is usually adopted to obtain the extreme values of the bending moment and shear force in the tunnel lining, whereas the no-slip assumption yields the maximum values of the thrust force acting on the lining. Since the shear force and the bending moment in full and no-slip conditions are slightly different ($10 \div 20\%$), while the thrust in no-slip condition can be much higher than in full-slip ($100 \div 200$ times), for the sake of conservationism the no-slip condition has just been assumed as the reference boundary condition.

The earthquake loading has been modeled as a uniform, quasi-static strain field simulating a pure shear deformation. This choice is justified by two reasons: firstly, the size of a typical lining cross-section is small compared with the wavelengths of the dominant ground motion producing the ovaling; secondly, the inertia effects in both the lining and the surrounding ground as produced by dynamic soil-structure interaction effects are relatively small (Penzien 2000). In an infinite medium, a strain field associated to a pure shear deformation can be obtained by applying a state of stress corresponding to an at-rest coefficient of lateral pressure K_0 equal to -1, as shown in Fig. 8.

The relations for displacements, bending moments, thrust and shear forces have been derived following the same approach used by Einstein and Schwartz (1979). However, the

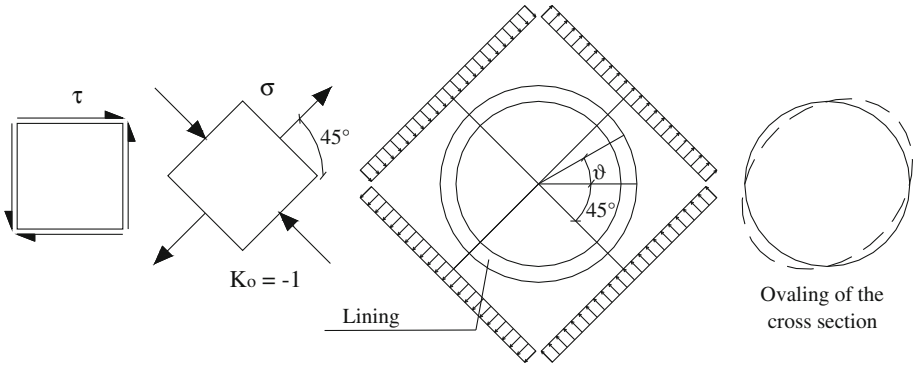

Fig. 8 State of stress around a tunnel corresponding to uniform, pure shear deformation

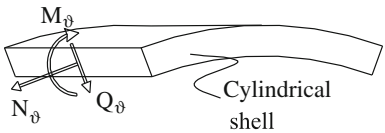

Fig. 9 Internal forces acting on the cylindrical shell in plane strain conditions

assumption that the induced internal forces are caused by excavation has been removed and replaced with an imposed, external quasi-static loading distribution to simulate the earthquake loading. The relationships derived for the thrust force (N_ϑ) and bending moment (M_ϑ) per unit length of tunnel lining (see Fig. 9) associated with the no-slip condition are the followings (Corigliano et al. 2006, Corigliano 2007):

$$N_\vartheta = \frac{E_g}{2\left(1+\nu_g\right)}\gamma_{ff\,\max} R\left(1-\frac{\delta}{3}\right)\cos\left[2\left(\vartheta+\frac{\pi}{4}\right)\right] \tag{4}$$

$$M_\vartheta = \frac{E_g}{2\left(1+\nu_g\right)}\gamma_{ff\,\max}\frac{R^2}{2}\left(1+\frac{\delta}{3}+\varepsilon\right)\cos\left[2\left(\vartheta+\frac{\pi}{4}\right)\right]. \tag{5}$$

In case of full slip condition these relations become respectively:

$$N_\vartheta = \frac{E_g}{2\left(1+\nu_g\right)}\gamma_{ff\,\max} R\ (1-2\eta)\cos\left[2\left(\vartheta+\frac{\pi}{4}\right)\right] \tag{6}$$

$$M_\vartheta = \frac{E_g}{2\left(1+\nu_g\right)}\gamma_{ff\,\max} R^2\,(1-2\eta)\cos\left[2\left(\vartheta+\frac{\pi}{4}\right)\right] \tag{7}$$

where the parameters ε, δ, η are defined by:

$$\varepsilon = \frac{\left\{2a\ \left[1+C^*\ \left(1-\nu_g\right)\right]-6\frac{C^*}{F^*}\ \ [a+4]\right\}}{a\ \left[4\ \nu_g-4-a\right]+3\ \frac{C^*}{F^*}\ \left\{4\ \nu_g+a-6\left(1-\nu_g\right)[2+a]\right\}+\left(1-2\nu_g\right)a} \tag{8}$$

with: $a = C^*\left(1-\nu_g\right)$;

$$\delta = \frac{a-2-\left[4\ \nu_g+a\right]\ \varepsilon}{2+a} \tag{9}$$

$$\eta = \frac{\left[F^*\left(1-\nu_g\right)+6\left(1/2-\nu_g\right)\right]}{\left[2F^*\left(1-\nu_g\right)+6\left(5-6\nu_g\right)\right]} \tag{10}$$

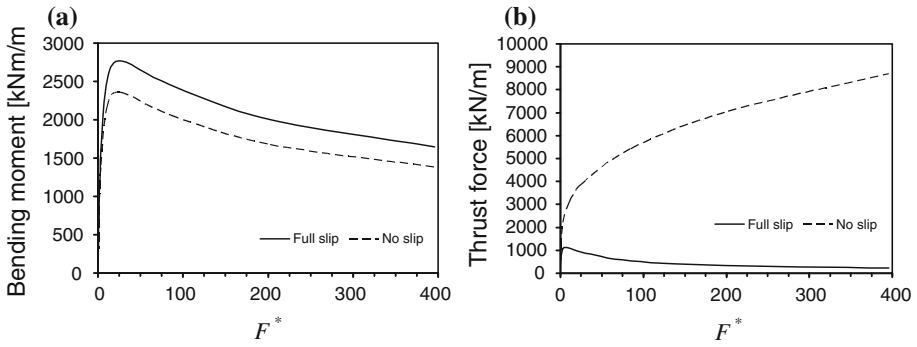

Fig. 10 Effect of the contact condition at the rock-mass-lining interfaces (full slip (*solid line*) and no slip (*dashed line*)) on the increment of the internal forces on the lining under seismic loading versus the flexibility ratio F*: **a** bending moment; **b** thrust force

where C^* and F^* are:

$$C^* = \frac{E_g R\left(1-\nu_s^2\right)}{E_s A_s\left(1-\nu_g^2\right)} \qquad F^* = \frac{E_g R^3\left(1-\nu_s^2\right)}{E_s I_s\left(1-\nu_g^2\right)}. \tag{11}$$

R is the average tunnel radius, A_s and I_s are the area and the moment of inertia per unit length of the lining, respectively, E_g, E_s, ν_g and ν_s are the Young's modulus and Poisson's ratio of ground and lining respectively. The parameters C^* and F^* are the "compressibility" and "flexibility" ratios. They represent a measure of the relative stiffness of the ground with respect to the supporting system (i.e. the lining) under a symmetric and antisymmetric loading respectively (Einstein and Schwartz 1979). Finally, ff max is the absolute value of maximum shear strain calculated in free-field conditions.

Closed-form solutions have the advantage to reflect the parameters that control the response of the system. Equations (4) through (7) show that the seismic response of the cross-section depends mainly on the relative stiffness of the lining with respect to the ground (through the parameter F^* for the earthquake loading), on the boundary condition at the ground support interfaces and on the maximum free-field shear deformation.

Figure 10 shows the effect of the relative stiffness and boundary conditions in terms of bending moment and thrust force, as function of the parameters F^*. From Fig. 10 it appears that the full-slip represents a slightly more critical boundary condition for the bending moment, whereas the no-slip provides the most critical assumption for the thrust force. It is also apparent from Fig. 10 that the full-slip condition under simple shear may cause significant underestimation of the maximum thrust force. Particularly, slip at the interface may be possible for tunnels in soft soils or in cases of severe seismic shaking. Since the real contact will be at an intermediate situation between the full-slip and the no-slip conditions, both cases should be investigated (Hashash et al. 2001).

Once the maximum shear strain induced during the seismic shaking ($\gamma_{ff\,\max}$) is known, the shear stress imposed at the boundary of the model can be easily computed using the theory of elasticity:

$$\sigma = \tau = \frac{E_g}{2\left(1+\nu_g\right)}\gamma_{ff\,\max} \tag{12}$$

where E_g and ν_g are the elastic parameters of the rock mass.

The key parameter for the definition of the state of stress in the tunnel lining is the free-field maximum shear strain. For the present case study, the earthquake-induced shear strain history γ_{yz} was calculated using Eq.(2), where displacement time histories $u(x, y)$ and $v(x, y)$ have been computed at four points along the lining of the cross-section (see Fig. 3) using the dynamic approach illustrated in Sect. 3.1. The maximum value of shear strain for free-field conditions turned out to be $\gamma_{ff\,\max} = 1.39 \times 10^{-4}$.

As a remark, it is noted that a simpler calculation of the maximum shear strain could have been performed using the simplified solution for earthquake-induced ground strain proposed by Newmark (1967) which relates the peak ground strain (*PGS*) to the peak particle velocity (*PGV*) through the formula $PGS = PGV/C$ (see Eq. 2). *PGV* has been computed using a ground motion prediction equation specifically developed for *near-field* conditions (e.g. Bray and Rodriguez-Marek 2004). The values obtained for PGV range from about 50–55 cm/s. Typical values for *C* range between 2 and 4 km/s (Abrahamson 2003). Setting this parameter to the lowest limit of 2 km/s, a value of $PGS = 1.30 \times 10^{-4}$ was obtained which is in very good agreement with the value predicted by the numerical simulations carried out suing the GRFLT program ($PGS = 1.39 \times 10^{-4}$).

Such a good agreement of the two solutions may be explained by the fact that the deformation field in this case-study generated by the earthquake scenario is dominated by wave propagation effects. A more complex rupture process would likely induce a larger degree of incoherence of ground motion, and consequently larger values of transient ground deformation.

A reasonable agreement has also been obtained between the closed-form solutions of the internal forces illustrated above and the results of numerical simulations (see Sect. 4.2). Figures 11a and b show the comparison in terms of bending moment and thrust force respectively. The thrust force calculated through the numerical analysis exceeds of about 30% the one computed analytically. The satisfactory agreement between the two solutions confirms that in near-fault conditions the inertial action is not relevant since the wavelength associated with the ground motion is larger than the cross-section of the tunnel.

It should be remarked that the bending moment and the thrust force shown in Fig. 11 represent the dynamic contribution. The total bending moment and thrust force are obtained by adding the dynamic increments to the static values as shown in Fig. 12. Theoretically, this linear superposition between static and dynamic phases is incorrect since the static phase may lead to concentration of stresses and non linear effects in some parts of the lining. However, it has been considered a reasonable assumption to compare the dynamic contribution with respect to the static case.

It turns out that, as a result of the severe earthquake scenario that it was assumed (it corresponds to a minimum recurrence period of about 2,000 years), the increase of the internal forces on the lining due to the seismic excitation almost leads to failure of the structural support (see Fig. 12). This outcome needs to be evidently taken into account when designing the lining of the tunnel. Thus, a proper design of a reinforced lined tunnel in seismically active regions requires a careful computation of the dynamic increment of the internal forces on the lining.

5 Concluding remarks

This paper attempted to provide a contribution into a better understanding of the seismic response of deep tunnels located in the vicinity of seismogenic faults using different methods of analysis. A specific case-study has been used to test and compare the various approaches.

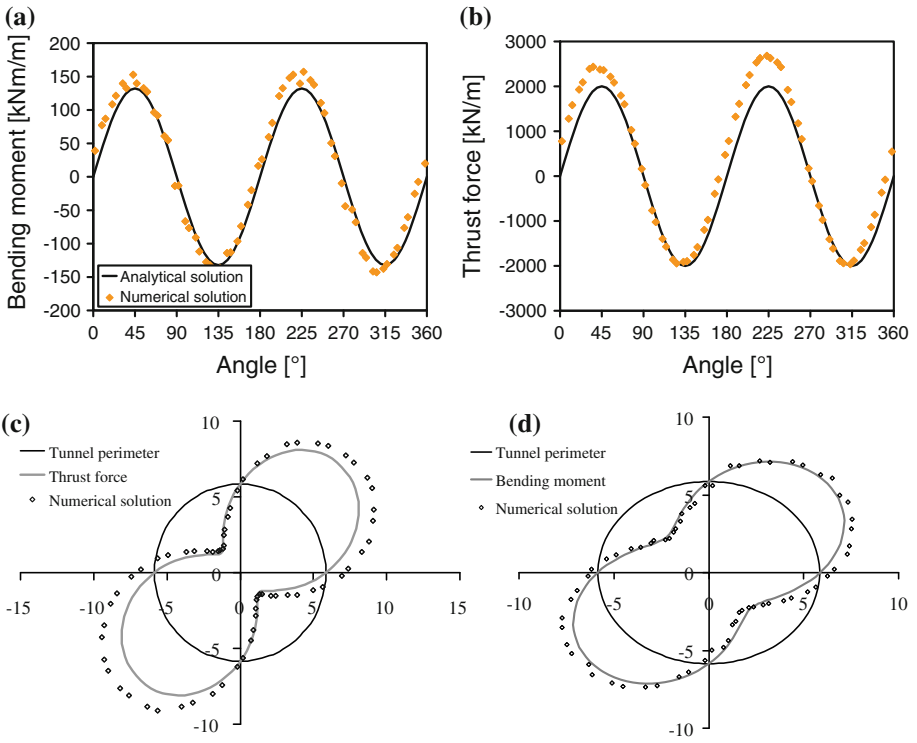

Fig. 11 Comparison between dynamic increment of internal forces evaluated by the numerical (rigorous (*squares*)) and analytical (simplified (*solid line*)) methods for the examined cross-section of the Serro Montefalco tunnel: **a** thrust force; **b** bending moment; **c** thrust force along the perimeter; **d** bending moment along the perimeter

This refers to a railway tunnel located in Southern Italy in a very active seismic territory. The static analysis of this underground structure predicts large values of stresses in the lining. As a result the tunnel is potentially vulnerable to the earthquake loading and the accuracy of the approach to determine the seismic stress increment is of paramount importance. Thus, a comprehensive study involving simulation of the effects of seismic source and propagation path accounting for near-source geological conditions and soil-structure interaction has been performed along the transversal direction of the underground structure by using the GeoELSE code, coupled with the Domain Reduction Method. Although the complexity of the problem has been increased, involving a large number of assumptions, from the characteristics of the seismic source, to the static and dynamic properties of the soil and the lining, this dynamic approach allowed us to check the reliability of simplified pseudo-static solutions.

Due to the large stiffness of the geomaterials where the tunnel is located, the propagating wavefield is characterized by wavelengths that are large with respect to the size of the lining. Under these conditions soil-structure interaction effects are negligible. The same conclusion does not generally apply to other tunnel configurations, such as shallow cut and cover tunnels, where the softer materials and the size of the cross-section may contribute to significant SSI effects.

A good agreement has been obtained from the comparison of the dynamic internal forces with those calculated using a pseudo-static simplified approach.

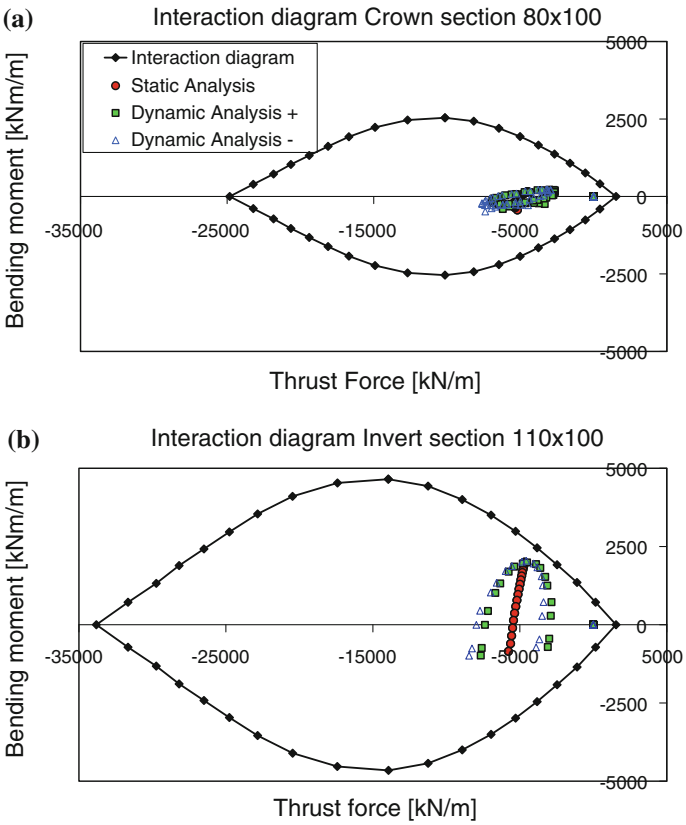

Fig. 12 Interaction diagram (*solid line with squares*) of the transversal cross-section of the Serro Montefalco tunnel at crown (**a**) and at invert (**b**), adding the dynamic stress increment as both a positive (*squares*) and negative (*triangles*) contributions to the static contribution (*circles*)

From the analyses along the transversal directions, it turned out that the estimation of the dynamic increment of the internal forces in the lining can be obtained in a simplified way by estimating the earthquake-induced ground strain assuming free-field conditions.

From this case study it can be concluded that simplified approaches for the seismic analysis of deep tunnels give reasonable results from an engineering point of view. Studies are currently under way to improve the reliability of simplified methods to compute the earthquake-induced maximum ground shear strain under free-field conditions to further facilitate the use of the pseudo-static approach in the seismic analyses of underground structures.

Acknowledgments The work presented in this paper was carried out with the financial support of the Department of Civil Protection (DPC) of Italian Government within the framework "Reluis-DPC—*Linea di Ricerca n. 6.2—Geotecnica Sismica—Costruzioni in Sotterraneo, Gallerie e Caverne in Roccia*" and by the Italian Ministry for Research and Higher Education (MiUR—Ministero dell'Università e della Ricerca) through the FIRB Project No. RBIN047WCL (Assessment and Reduction of Seismic Risk to Large Infrastructural Systems) whose contribution is greatly acknowledged. The authors wish to thank the coordinator of the line 6.2 of the Reluis project Prof. Giovanni Barla (Politecnico di Torino)

References

Abrahamson NA (2003) Model for strains for transient ground motion. In: Proceedings of the workshop on the effects of earthquake-induced transient ground surface deformations at-grade improvements. CUREE. N. EDA-04, Oakland, CA, USA. http://www.curee.org/projects/EDA/docs/CUREE-EDA04.pdf

AFPS/AFTES (2001) Earthquake design and protection of underground structures

Ates Y, Bruneau D, Ridgway WR (1995) An evaluation of potential effects of seismic events on a used fuel disposal fault. AECL TR-623 86 p, AECL

Barla G, Caruso G, Rondini G (1986) La problematica delle gallerie nel raddoppio della linea ferroviaria Caserta-Foggia. Congresso internazionale su grandi opere sotterranee, Firenze, Italy

Barton N (1984) Effects of rock mass deformation on tunnel performance is seismic regions. Adv Tunn Tech Subsurf Use 4:89–99

Bielak J, Loukakis K, Hisada Y, Yoshimura C (2003) Domain reduction method for three-dimensional earthquake modeling in localized regions part I: theory. BSSA 93(2):817–824

Bray JD, Rodriguez-Marek A (2004) Characterization of forward-directivity ground motions in the near fault-region. Soil Dyn Earthq Eng 24:815–828

Corigliano M, Scandella L, Barla G, Lai CG, Paolucci R (2007) Seismic analysis of deep tunnels in rock: a case study in Southern Ital. In: 4th international conference on earthquake geotechnical engineering. Paper 1616

Corigliano M (2007) Seismic response of deep tunnels in near-fault conditions. PhD dissertation, Politecnico di Torino, Italy, p 222

Corigliano M, Lai CG, Barla G (2006) Seismic response of rock tunnels in near-fault conditions. In: 1st European conference on earthquake engineering and seismology. September 3–8, Geneva, Switzerland, Paper 998

Cotton F, Scherbaum F, Bommer JJ, Bungum H (2006) Criteria for selecting and adjusting ground-motion models for specific target regions: application to Central Europe and rock sites. J Seismol 10:137–156

DISS v. 3.0.3 (2006) Database of individual seismogenic sources: a compilation of potential sources for earthquakes larger than M 5.5 in Italy and surrounding areas. http://www.ingv.it/DISS/

Einstein HH, Schwartz CW (1979) Simplified analysis for tunnel support. J Geotech Eng Div 105:499–518

Erdik M (2000) Report on 1999 Kocaeli and DŸzce (Turkey) earthquakes. In: Proceedings of the second Euro-conference on global change and catastrophe risk management: earthquake risks in Europe, Laxenburg, Austria. Reference: http://www.iiasa.ac.at/Research/RMS/july2000/Papers/erdik.pdf

Eurocode 8 (2004) Design of structures for earthquake resistance. Part 1: general rules, seismic actions and rules for building. EN 1998-1, December 2004, Comité Européen de normalisation, Brussels

Faccioli E, Maggio F, Paolucci R, Quarteroni A (1997) 2D and 3D elastic wave propagation by a pseudo-spectral domain decomposition method. J Seismol 1:237–251

Faccioli E, Vanini M, Paolucci R, Stupazzini M (2005) Comment on "Domain reduction method for three-dimensional earthquake modeling in localized regions, part I: theroy," by J. Bielak, K. Loukakis, Y. Hisada, and C. Yoshimura, and "part II: verification and applications," by C. Yoshimura, J. Bielak, Y. Hisada, and A. Fernández. Bull Seism Soc Am 95(2):763–769

Hashash YMA, Hook JJ, Schmidt B, Yao JIC (2001) Seismic design and analysis of underground structures. Tunn Undergr Space Technol 16:247–293

Hashash YMA, Park D, Yao JIC (2005) Ovaling deformations of circular tunnels under seismic loading, an update on seismic design and analysis of underground structures. Tunn Undergr Space Technol 20: 435–441

Hisada Y, Bielak J (2003) A theoretical method for computing near fault ground motion in a layered half-spaces considering static offset due to surface faulting, with a physical interpretation of fling step and rupture directivity. Bull Seism Soc Am 93(3):1154–1168

Improta L, Iannaccone G, Capuano P, Zollo A, Scandone P (2000) Inferences on the upper crustal structure of Southern Apennines (Italy) from seismic refraction investigations and subsurface data. Tectonophysics 317:273–297

ISO 23469 (2005) Bases for design of structures—seismic actions for designing geotechnical works

Itasca (2005) FLAC (Fast Lagrangian analysis of continua): user's guide. Itasca Consulting Group, Inc., Minneapolis

Kontoe S, Zdravkovic L, Potts DM, Menkiti CO (2008) Case study on seismic tunnel response. Can Geotech J 45:1743–1764

Lunardi P, Bindi R (2004) The evolution of reinforcement of the advanced core using fibre-glass elements. FELSBAU J Eng Geol Geomech Tunn 4:8–19

Newmark NM (1967) Problems in wave propagation in soil and rocks. In: Proceedings of the international symposium on wave propagation and dynamic properties of earth materials. University of New Mexico Press, pp 7–26

NTC—Norme Tecniche per le Costruzioni—DM 14/01/2008

O'Rourke MJ (2003) Buried pipelines, earthquake engineering handbook charter 23. CRC Press, Boca Raton

Oreste PP (1999) Aspetti notevoli dell'analisi e dimensionamento dei sostegni di gallerie. Gallerie e opere in sotterraneo

Panet M (1995) Le Calcul des Tunnels par la Méthode Convergence-Confinement. ENPC, Paris

Paolucci R, Pitilakis K (2007) Seismic risk assessment of underground structures under transient ground deformations. In: Earthquake geotechnical engineering, 4th international conference on earthquake geotechnical engineering—invited lectures, Thessaloniki, Greece. Springer, Berlin, pp 433–459

Paolucci R, Smerzini C (2008) Earthquake-induced transient round strains from dense seismic networks. Earthq Spectra 24(2):453–470

Penzien J (2000) Seismically induced racking of tunnel linings. Earthq Eng Struct Dyn 29:683–691

Scandella L, Paolucci R (2010) Earthquake induced ground strains in the presence of strong lateral soil heterogeneities. Bull Earthq Eng. Published on line, 23 May 2010

Scandella L (2007) Numerical evaluation of transient ground strains for the seismic response analysis of underground structures. PhD Thesis, Politecnico di Milano

Stupazzini M, Paolucci R, Igel H (2009) Near-fault earthquake ground motion simulation in the Grenoble Valley by a high-performance spectral element code. Bull Seismolog Soc Am 99(1):286–301

Stupazzini M, Paolucci R, Scandella L, Vanini M (2006) From the seismic source to the structural response: advanced modelling by the spectral element method. In: 1st European conference of earthquake engineering and seismology, Genève, September 2006

Wang JN (1993) Seismic design of tunnels: a state-of-the-art approach. Parsons Brinckerhoff Quade e Douglas, Inc., New York, Monograph 7

Zerva A (2003) Transient ground strains: estimation, modeling and simulation. In: Workshop Proceedings on the effect of earthquake-induced transient ground surface deformations on at-grade improvements, May 28 2003, Oakland, CA, USA